NUMERICAL SIMULATION OF NATURAL CONVECTION IN AN OBLIQUE ENCLOSURE FILLED WITH SILVER –WATER NANOFLUID

Mr. Farooq Hassan Ali

College of Engineering-Mechanical Engineering Department

Babylon University - Babylon City – Hilla – Iraq.

Email: farooq_hassan77@ yahoo.com

Received 22 September 2015 Accepted 9 November 2015

ABSTRACT

In this work, a numerical simulation of natural convection in an oblique enclosure filled with silver-water nanofluid is obtained for different values of Rayleigh numbers, volume fraction and inclination angle of sloping walls. The considered oblique enclosure with left and right side walls are maintained at constant cold temperature (T_c). The horizontal top wall of enclosure is kept insulated, but the bottom is maintained at constant hot temperature (T_h). The present work is utilized to obtain results in the range of Rayleigh number (10^3-10^6) , volume fraction of nanofluid varied from (0-0.2) and inclination angle of side walls are (-60^o, -30^o, 0^o, 30^o, 60^o). The Prandtle number is 6.0. The governing equations in the two-dimensional are solved numerically by using finite-difference technique.

Comparisons with other works are performed and the results are found to be in good agreement. The obtained results are shown in the form of stream function, isothermal lines and average Nusselt numbers. It observed from results that acute shaping wall and Ag-nanoparticles with high concentration are effective to enhance the rate of heat transfer, also; the average Nusselt number for all range of inclination angle increases with increase in the Rayleigh number and the solid volume fraction of the Nanofluid.

***K*eywords:** Natural Convection, Oblique Enclosure, Nanofluid, Rayleigh Number

النمذجة العددية للحمل الحر في حيز مائل مملوء بمائع الفضة النانوي

م. فاروق حسن علي

الخلاصة.

تمت دراسة الحمل الحر في حيز مائل يحتوي على مائع الفضة النانوي لقيم مختلفة من ارقام رالي، الحجم الجزئي، زاوية ميلان الجدار. اعتبرت الجدران الجانبية المائلة الايمن والايسر للحيز عند درجة حرارة باردة. الجدار الافقي الاعلى اعتبر معزولا، بينما كان الجدار الافقي الاسفل عند درجة حرارة ساخنة. كان رقم رالي يتراوح بين(10^3-10^6)، بينما تراوح الحجم الجزئي بين (0-0.2) وتراوحت زاوية ميلان الجدران الجانبية بين (-60^o, -30^o, 0^o, 30^o, 60^o). وكان رقم برانتل يساوي 6.0. تم حل المعادلات الحاكمة لبعدين عدديا باستخدام تقنية الفروقات المحددة.

جرت المقارنة مع بحوث سابقة واظهرت النتائج تطابق جيد. مثلت نتائج هذه الظاهرة بدالة الجريان، خطوط الحرارة وارقام نسلت. لقد لوحظ من النتائج ان للزوايا الحادة للجدار واضافة مائع النانوي بتراكيز عالية الاثر الكبير في تعزيز انتقال الحرارة، كذلك ان متوسط رقم نسلت لجميع زوايا الميلان يزداد بزيادة رقم رالي وكذلك زيادة تركيز المائع النانوي.

NOMENCLATURE:

Symbol	Description	Unit
C_p	*Specific heat*	*kJ/kg.K*
g	*Gravitational acceleration*	m/s^2
H	*Height of the parallelogram cavity*	*m*
K	*Thermal conductivity of fluid*	*W/m.K*
N	*Outward flux normal to boundary*	
Nu	*Average Nusselt Number*	
P	*Dimensionless pressure*	
P	*pressure*	
$Pr = \nu / \alpha$	*Prandtl Number*	
$Ra = g\beta qL^5 / \alpha\nu k$	*Rayleigh Number*	
S	*Nondimensional length along inclined heated surface*	
T	*Temperature*	*K*
T_C	*Temperature of the cold surface*	*K*
T_H	*Temperature of the hot surface*	*°C*
u	*Velocity component in x-direction*	*m/s*
U	*Dimensionless velocity component in x-direction*	
v	*Velocity component in y-direction*	*m/s*
V	*Dimensionless velocity component in y-direction*	
x	*Cartesian coordinate in horizontal direction*	*m*
X	*Dimensionless cartesian coordinate in horizontal direction*	
y	*Cartesian coordinate in vertical direction*	*m*
Y	*Dimensionless cartesian coordinate in vertical direction*	
Greek Symbols		
α	*Thermal diffusivity*	m^2/s
β	*Volumetric coefficient of thermal expansion*	K^{-1}
θ	*Dimensionless temperature*	
μ	*Dynamic viscosity of the fluid*	$N.s/m^2$
φ	*Nanoparticles volume fraction*	
ϑ	*Kinematic Viscosity of the Fluid*	m^2/s
ρ	*Density of the fluid*	kg/m^3
Φ	*Sidewall inclination angle from vertical*	*deg*
ψ	*Dimensionless stream function*	

Ψ	*Stream function*	m^2/s

Subscripts

C	*Cold*
f	*Fluid (pure)*
nf	*nanofluid*
H	*Hot*
s	*Solid (nanoparticale)*
L	*Left sidewall*
R	*Right sidewall*

Abbreviation

Fig	*Figure*
FDM	*Finite difference method*
min	*Minimum*
max	*Maximum*

1- INTRODUCTION

In the last decade, a computational as well as experimental researches have analyzed the natural convection heat transfer phenomena with addition of fluid suspension of Nano metric solid particles or fibers to the liquids. These addition effect on the performance of the heat of the liquids. The steady state natural convection heat transfer characteristics in a differentially heated square enclosure filled with different types of nanofluids for different published variables have been investigated in the literature **[1-5]**. Moreover, the unsteady state natural convection heat transfer of water-Al_2O_3 nano fluid in differentially heated square enclosure too, is studied numerically by **T. A. AL-Hattab [6]** using a finite element method. Also, for the above-mentioned diversity among the numerical predictions but the work of **Y. varol et. al. [7]** and **C. J. Ho et. al. [8]**, an experimental studies have been undertaken concerning natural convection heat transfer efficacy of using nanofluids in an enclosures.

In the recent years, the Lattice Boltzmann simulation were applied to investigate the natural convection flow utilizing nan fluid. **Fattahi et. al. [9]** and **GH. R kefayati et. al.[10]** applied the Lattice Boltzmann method to investigate the natural convection flow utilizing Al_2O_3 or Cu-water, and Sio_2-water nanofluids respectively, in a square cavities. The results indicates that by increasing volume fraction, the average Nusselt numbers increase for all used nanofluids. As well as the same results of average Nusselt numbers were obtained by **GH. R. Kefayti et. al. [11]** investigation by using Lattice Boltzmann simulation of natural convection in an open enclosure which subjected to Cu-water nanofluid. In addition a Lattice Boltzmann model is developed by **Y. He. et. al. [12]** by coupling the density and the temperature distribution to simulate the convection heat transfer utilizing Al_2O_3-water nanofluids in a square cavity. Inclination angle and sinusoidal heating or cooling can be a control parameters and percentage enhancement of heat transfer for nanofluid filled enclosure. Hence **H. F. Oztop et. al. [13]** and **H. K. Oztop et. al. [14]**, analyzed numerically the effect of inclination angle and a sinusoidal heating and cooling temperature profiles on one side, respectively, on natural convection heat transfer and fluid flow in a two-dimensional enclosure filled with nanofluid. Also, **E. B. Ogut [15]** investigate the natural convection heat transfer of water based in a nanofluid in inclined square enclosure where left vertical side is heated with a constant heat flux. The result show that the length of the heater is also important parameter affecting on the flow and temperature fields. A comparison studied were presented by **S. M. Aminosadti** and **B. Ghasmi [16-18]** and **S. M. Aminosadti** and **B. Ghasmi [19]** for multi cases of heat transfer in the nanofluid filled a square and triangular cavities respectively

with different arrangement and oscillation of the one or two heat source-sink on the walls of the cavities. The result show that the length, location, oscillation of the source and the shape of the cavity proved to significant design of an effective cooling system for electronic components to help ensure, effective and safe operation conditions.

Natural convection inside irregular and non-square enclosures has a wide applications in engineering and industry. Investigation on natural convection in non-square enclosure with different geometries has been done by many researches. Hence, the works of **M. Mohmoodi [20-21]** and **H. Saleh et. al. [22]** focus on problems of free convection fluid and heat transfer of a nanofluid inside L-shaped and trapezoidal cavities, respectively. The obtained results for L-shaped enclosure show that the average Nusselt number increases with increase in the Rayleigh number for all range of enclosure aspect ratio. Moreover, it is found that the rate of heat transfer increases with decreasing the aspect ratio of the enclosure. Also, it was found for trapezoidal enclosure that acute shaping wall and Cu- nanofluid with high concentration are effective to enhance the rate of heat transfer.

Six common enclosures shapes are investigated by **O. Abouali et. al. [23]** to show that the internal natural convection of a single phase nanofluids in enclosures can be easily predicted theoretically with no need to perform a numerical solution. **Habibis et. al. [24]** carried out a numerical investigation on heat transfer enhancement utilizing Cu-water nanofluid in a parallelogrammic enclosure by finite difference method. The result show that increasing the base angle caused decreasing the heat transfer rate.

Finally, laminar natural convection of a copper-water nanofluid in differentially heated parallelogrammic enclosure has been studied numerically using the finite volume method by **Salam et. al. [26]** the result show that the heat transfer rate increase remarkably by the addition of copper-water nanofluid and the shape of the convection vortices is sensitive to the skew angle variation.

Based on literature reviews, a little effort has been spent up to date to simulate the natural convection heat transfer in an oblique enclosures filled with nanoparticles. This problem may be happened in many applications such as cooling or heating of electronic device. In the present work the of natural convection heat transfer and fluid flow in oblique enclosure filled with silver-water nanofluid is investigated numerically using the finite difference method. The results are shown in the forms of streamlines, isotherms plots and average Nusselt numbers for three walls, right, left and bottom, wide range of Rayleigh numbers (10^3-10^6) are presented and the effect of the oblique enclosure angles are considered also between ($-60^o<\Phi<60^o$).

2- Governing equations and boundary conditions

Fig.1 shows a schematic configuration of the computational domain and coordinate system used in the present study. Governing equations and boundary conditions of two-dimensional natural convection steady, laminar and incompressible of a silver-water inside oblique enclosure are describe below.

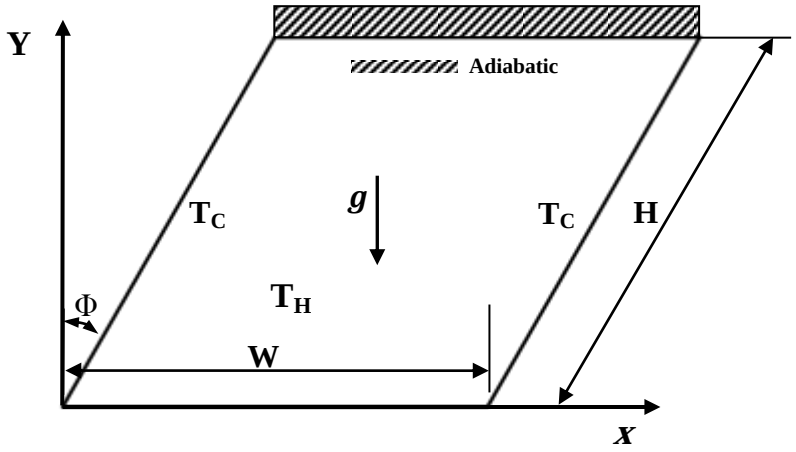

Figure (1): Schematic diagram and coordinate system of the physical domain with boundary conditions.

The dimensionless forms of the governing equations (continuity, momentum and energy equations) for the present problem can be written as follows[13]:

$$\frac{\partial \mathrm{U}}{\partial \mathrm{X}} + \frac{\partial \mathrm{V}}{\partial \mathrm{Y}} = 0 \tag{1}$$

$$U\frac{\partial U}{\partial X} + V\frac{\partial U}{\partial Y} = -\frac{\rho_f}{\rho_{nf}}\frac{\partial P}{\partial X} + Pr\frac{\vartheta_{nf}}{\vartheta_f}\left(\frac{\partial^2 U}{\partial X^2} + \frac{\partial^2 U}{\partial Y^2}\right) \tag{2}$$

$$\mathrm{U}\frac{\partial \mathrm{V}}{\partial \mathrm{X}} + \mathrm{V}\frac{\partial \mathrm{V}}{\partial \mathrm{Y}} = -\frac{\rho_{\mathrm{f}}}{\rho_{\mathrm{nf}}}\frac{\partial \mathrm{P}}{\partial \mathrm{Y}} + \mathrm{Pr}\frac{\vartheta_{\mathrm{nf}}}{\vartheta_{\mathrm{f}}}\left(\frac{\partial^2 \mathrm{V}}{\partial \mathrm{X}^2} + \frac{\partial^2 \mathrm{V}}{\partial \mathrm{Y}^2}\right) + \mathrm{Ra}\ \mathrm{Pr}\ \frac{(\rho\beta)_{\mathrm{nf}}}{\rho_{\mathrm{nf}}\beta_{\mathrm{f}}}\ \theta \tag{3}$$

$$\mathrm{U}\frac{\partial \theta}{\partial \mathrm{X}} + \mathrm{V}\frac{\partial \theta}{\partial \mathrm{Y}} = \frac{\alpha_{\mathrm{nf}}}{\alpha_{\mathrm{f}}}\left(\frac{\partial^2 \theta}{\partial \mathrm{X}^2} + \frac{\partial^2 \theta}{\partial \mathrm{Y}^2}\right) \tag{4}$$

Where

$$\theta = \frac{T - T_C}{T_H - T_C}, X = \frac{x}{H}, Y = \frac{y}{H}, U = \frac{u\,H}{\alpha_f}, V = \frac{v\,H}{\alpha_f}, \psi = \frac{\Psi}{\alpha_f}, P = \frac{p\,H^2}{\rho_{nf}\ \alpha_f^2}, Pr = \frac{\vartheta}{\alpha}, and$$

$$\mathrm{Ra} = \frac{g\beta_f(T_H - T_C)H^3}{\vartheta_f \alpha_f}$$

Thermal diffusivity, the effective density and heat capacity of nanofluids given as [13]:

$$\alpha_{nf} = k_{nf}/(\rho c_P)_{nf} \tag{5}$$

$$\rho_{nf} = (1 - \varphi)\rho_f + \varphi\,\rho_s \tag{6}$$

$$(\rho c_P)_{nf} = (1-\varphi)(\rho c_P)_f + \varphi(\rho c_P)_s \quad (7)$$

Furthermore, the effective thermal expansion coefficient (β_{nf}) and viscosity of nanofluid (μ_{nf}) were introduced as below [13]:

$$(\rho\beta)_{nf} = (1-\varphi)(\rho\beta)_f + \varphi(\rho\beta)_s \quad (8)$$

$$\mu_{nf} = \frac{\mu_f}{(1-\varphi)^{2.5}} \quad (9)$$

In addition, the effective thermal conductivity (k_{nf}) of nanofluid is approximated by the Maxwell-Garnetss [25]:

$$\frac{k_{nf}}{k_f} = \frac{k_s + 2k_f - 2\varphi(k_f - k_s)}{k_s + 2k_f + \varphi(k_f - k_s)}$$

The fluid motion is displayed using the dimensionless stream function (ψ) obtained from velocity components U and V. The relationships between stream function and velocity components for two dimensional flows are:

$$U = \frac{\partial\psi}{\partial Y}, V = -\frac{\partial\psi}{\partial X} \quad (10)$$

According to Fig.1 the boundary conditions as applied in this present simulation are:

At the left wall: *U=0, V=0, T=*T_c

At the right wall: *U=0, V=0, T=*T_c

At the top wall: *U=0, V=0,* $\frac{\partial T}{\partial x} = 0$

At bottom wall: *U=0, V=0, T=*T_H

The rate of heat transfer is represented in terms of average Nusselt number at the side walls $(\overline{Nu}_{\text{L or R}})$ as follows:

$$\overline{Nu}_{\text{L or R}} = -\frac{1}{S}\int_0^S \left(\frac{k_{nf}}{k_f}\right)\left[\frac{\partial\theta}{\partial n}\right]_{X=0} dn \quad (11)$$

Where S and n are the non-dimensional length and coordinate along the inclined walls respectively.

3- NUMERICAL SOLUTION

The discretization procedure of the governing equations is based on a finite difference technique. A non-uniform finite difference mesh with collocated variable locations is used for the computation. The set of governing equations are integrate over the finite differences, which produces a set of linear algebraic equations. The convection term are discretized using the second-order upwind scheme while the diffusion terms are discretized using the central difference scheme. The pressure

velocity coupling is treated using the well-known SIMPLEC method. The set algebraic equations for each variable are solved sequentially using an iterative method. The solution is considered converged when the normalized residual falls below 10^{-6} for the energy equation and below 10^{-4} for other variables. The stricter convergence limit for the energy equation is required to ensure global heat balance. To validate the numerical simulation, the results present work of natural convection in a square enclosure were compared with the previous published works of Basak and Chemka [4]. It is worth mentioning that the side walls are fixed at cold temperature (T_C). The horizontal top wall is insulated but the bottom are fixed too at hot temperature (T_H). We use the same boundary conditions and wall temperatures on horizontal and vertical walls of the enclosure. Streamlines and isotherms for different values of Rayleigh number (Ra= 10^3 and 10^5) are presented in Fig.2. It can be seen from the figure that the present results and those reported by Basak and Chemka [4] are in excellent agreement.

4- RESULTS AND DISCUSSIONS

The natural convection of silver-water nanofluid is investigated for various value of Rayleigh numbers and volume fractions in oblique enclosure. The Rayleigh number varied from (10^3-10^6) and volume fraction from (0-0.2) while the oblique angle changed from (-60^o to 60^o). Water is the base fluid with Pr=6.57 at 22^{o}C, containing Ag nanoparticles.

Figs. (3&4) show the contours for the stream function and temperature respectively for Ag-water nanofluid for different oblique angle (Φ) and Rayleigh number at volume fraction (φ=0) and (φ=0.15). This figures illustrates the effects of Rayleigh number and side wall inclination angle for pure water (φ=0) and volume fraction (φ=0.15) nanofluid.Fig.3 shows that when (Φ=0) and (Ra=10^3), symmetrical flow and temperature pattern are observed in enclosure since the symmetric boundary conditions along middle horizontal axis, two large recirculating eddies with elliptical-shaped core region are generated inside the enclosure as a result of cooling nanofluid along cold side walls and heating nanofluid parallel to the hot bottom wall. Also seen from figure (3) with increase of Rayleigh number from 10^4 to 10^6, the flow pattern does not change significantly and the shape of the central region of eddies, which are ellipses, does not change. The value of stream function increases, more over the maximum stream function is seen toward the core region of the two eddies due to the increase of the heat transfer from hot bottom wall and fluid since velocity increase.

The effect of change in inclination angles can be more clearly understood from contours plots (second and third columns), when (Φ=30^o) the right cell becomes more elongate and penetrates into acute corner of the enclosure, with increasing Rayleigh number the right cell squeeze along the cold right wall and expand along the hot bottom wall and two small cells appears along the left side wall because the convective mode was dominated in the enclosure. For (Φ=60^o) two cells occupied the enclosure, with increase Rayleigh number right cell becomes large in size while left cell becomes small in size because convective is dominated. In general, the effect of nanoparticles on the streamlines is clear when the value of the maximum stream function and stream lines motivation reduced for different Rayleigh number, but no significant change in flow patterns is observed.

Fig.(4) show the temperature contours for Ag-water nanofluid for different oblique angle (Φ) and Rayleigh number at volume fraction (φ=0) and (φ=0.15), when (Φ=0^o) thermal distribution reflect the conduction heat transfer mode. with increase in the Rayleigh number, convection heat transfer becomes stronger. In addition, the temperature contours becomes more and more crowded near the cold side walls as Rayleigh number increases, which explains that the heat transfer behaviors change from conduction to convection. It should be marked that the thermal boundary layer at the cold walls decreases as the inclination angle is increased and increases with the Rayleigh number is increased. With the increment of the tilting angle, the isotherms near the left acute angle becomes proximate and rigorous plum formation as Rayleigh number increased. Since the increase in the

viscosity of the nanofluid with the increase the volume fraction, the diffusion of heat transfer is increased, therefore the crowded of temperature contours near the side walls decrease.

Fig. (5) illustrates the stream function for various values of Ra= 10^3, 10^4, 10^5 and 10^6 and twice skew angles(-30^o) and (-60^o) at volume fraction φ=0.15. For pure water (dotty lines) and Ag-nanofluid (solid lines). It is noticed at low Rayleigh number the enclosure filled by two cells, left large cell and right small cell. This configuration appears since the distribution of boundary conditions and inclination angles. As expected due to the cold vertical walls, fluids rise up from middle portion of the bottom wall and flow down along the two vertical walls forming two unsymmetrical cells with clock and anti-clockwise direction inside the enclosure. At lower Rayleigh number, the magnitude of stream function are considerably lower (ψ_{max}=0.135 for Φ=-30o and ψ_{max}=0.045 for Φ=-60^o) and conduction heat transfer mode was dominant. Also it can be observed that the behavior of pure water and nanofluid are identical for the same reason. When Rayleigh number increase this identical was vanished since the convection mode becomes dominant and velocity of fluid increasing. The difference in density between pure and nanofluid makes this dissimilarity in flow pattern between them.

Effect of negative inclination angle of the sloping walls on the thermal filed are presented in Fig.6, for water-Ag nanofluid with volume fraction (φ=0.15) and pure water with the range of Rayleigh number (Ra=10^3-10^6). The isothermal lines are smooth curves with respect to the vertical lines, with increasing gradually and the advection takes the command, becoming the dominant mode of heat transfer. The circulation is greater near the center and least at the wall due to no slip boundary condition. It is observed from isothermal lines the nanofluid lines take the same habit as pure water at low Rayleigh number but this habit vanish and interaction between isothermal lines of nanofluid and pure fluid take placed due to advection effect.

The average mean Nusselt number variation across left cold wall, right cold wall and bottom hot wall for different inclination angles and Rayleigh values are shown from Fig. (7) to Fig. (11).Five different volume fraction are used as φ=0, 0.05, 0.1, 0.15 and 0.2 . Average Nusselt number is calculated by integration of local Nusselt number over walls surfaces as given in equation (12). For all figures subscript (a, b, c) refers to the average Nusselt number over the left, right and bottom walls respectively. As given in the figures, average Nusselt number are almost constant up to Ra=10^4 due to quasi-conductive regime, after that they increasing with increasing Rayleigh number as expected. For all values of volume fraction and skew angles the same trend are noticed. For each graph when compared with each other, it is seen that, Nusselt number is increased with increasing of volume fraction due to increase the thermal conductivity of nanofluid which causes more heat transfer passes.Fig.(12) shows profiles of the average Nusselt number along the bottom heated wall versus the inclination angle for silver nanofluids at volume fraction (φ=0.2) and a range of Rayleigh number ($10^3 \leq Ra \leq 10^6$). Symmetrical trends are noticed also the enhance heat transfer rate more evident at the parallelogram geometry ($\Phi=60^o$ and -60^o) than the square geometry ($\Phi=0^o$). this is due to that at parallelogram geometry the inclination sidewalls have large surface area this lead to high heat transfer rate.

5- CONCLUSIONS

In this numerical analysis the results of the study of natural convection in an oblique enclosure filled with silver-water nanofluid are presented using parameter of interest as Rayleigh number, volume fraction and angle of inclination.

In view of the obtained results, the following findings may be summarized:

(1) Average Nusselt number becomes constant for the smaller value of Rayleigh numbers due to domination of conductive regime.

(2) It is observed that the volume fraction and skew angles are one of the most importance parameters on the flow fields, temperature fields and heat transfer.

(3) Increased volume fraction percentage, as expected, enhances the heat transfer due to increasing thermal conductivity as can observed in table (1).

(4) Peak values on average Nusselt number distribution are observed on the hot bottom wall, with addition of the nanofluid and increasing Rayleigh number when the angle of inclination equal (60^o, -60^o). This is due to the high amount of flow velocity.

(5) The flow intensity increases as the volume fraction and Rayleigh number increases and reaches maximum at parallelogram shape ($\Phi=60^o$ and -60^o) and reaches minimum at square shape ($\Phi=0^o$).

References

[1] Ayad M. Salman; An investigation of natural convection heat transfer in a square enclosure filled with nanofluid, Eng. & Tech. Journal, Vol.29, No.12 (2011) 2346-2363.

[2] Mehdi Nikfar, Mustafa Mahmoodi; Meshless local Petrov-Galerkin analysis of free convection of nanofluid in a cavity with wavy side walls, Engineering Analysis with Boundary Elements 36 (2012) 433-445.

[3] Eiyad Abu-Nada, Ali J. Chamkha; Effect of nanofluid variable properties on natural convection in enclosures filled with a CuO-EG-water nanofluid, International Journal of Thermal Science 49 (2010) 2339-2352.

[4] Tanmay Basak , Ali J. Chamkha; Heatline analysis on natural convection for nanofluid confined within square cavities with various thermal boundary conditions, International Journal of Heat and Mass Transfer 55 (2012) 5526–5543.

[5] W. Rashmi, A. F. Ismail, M. Khalid, Y. Faridah; CFD studies on natural convection heat transfer of Al_2O_3-water nanofluid, Heat Mass Transfer 47 (2011) 1301-1310.

[6] Tahseen A. Al-Hattab; Transient free convection of Al_2O_3 nanofluid in a square cavity , The 7^{th} Jordanian Mechanical Engineering Conference (2010).

[7] Yasin Varol, Hakan F. Oztop, Filiz Ozgen, Ahmet Koca; Experimental and numerical study on laminar natural convection in a cavity heated from bottom due to inclined fin, Heat Mass Transfer (2011).

[8] C. J. Ho, W. K. Liu, Y. S. Chang, C. C. Lin; Natural convection heat transfer of alumina-water nanofluid in vertical square enclosure: An experimental study, International Journal of Thermal Sciences 49(2010) 1345-1353.

[9] Ehsan Fattahi, Mousa Farhadi, Kurosh Sedighi, Hasan Nemati; Lattice Boltezmann simulation of natural convection heat transfer in nanofluids, International Journal of Thermal Science 52(2012) 137-144.

[10] GH. R. Kefayati, S. F. Hosseinizadeh, M. Gorji, H. Sajjadi; Lattice Boltezmann simulation of natural convection in tall enclosure using water-SiO2 nanofluid, International Communication in Heat and Mass Transfer 38 (2011) 798-805.

[11] GH. R. Kefayati, S. F. Hosseinizadeh, M. Gorji, H. Sajjadi; Lattice Boltezmann simulation of natural convection in an open enclosure subjected to water/copper nanofluid, International Journal of Thermal Science 52 (2012) 91-101.

[12] Yureng He, Cong Qin, Yanwei Hu, Bin Qin, Fengchen Li, Yulon Ding; Lattice Boltzmann simulation of alumina-water nanofluid in a square cavity, Nanoscale Research Letters (2011).

[13] Eiyad Abu-Nada, Hakan F. Oztop; Effect of inclination angle on natural convection in enclosure filled with Cu-water nanofluid, International Journal of Heat and Fluid Flow, 30 (2009) 669-678.

[14] Hakan F. Oztop, Eiya Abu-Nada, Yasin Varol, Khaled Al-Salem; Computational analysis non-isothermal temperature distribution on natural convection in nanofluid filled enclosures, Superlattices and Microstructure 49 (2011) 453-467.

[15] Elif Buyuk Ogut; Natural convection of water-based nanofluids in inclined enclosure with a heat source, International Journal of Thermal Sciences 48 (2009) 2063-2073.

[16] S. M. Aminossadati, B. Ghasmi; Natural convection cooling of a localized heat source at the bottom of a nanofluid-filled enclosure, European Journal of Mechanics B/Fluids 28(2009) 630-640.

[17] S. M. Aminossadati, B. Ghasemi; Natural convection of water-CuO nanofluid in a cavity with two pairs of heat source-sink, International Communication in Heat and Mass Transer 35 (2011) 672-678.

[18] B. Ghasemi, S. M. Aminossadati; Periodic natural convection in a nanofluid-filled enclosure with oscillating heat flux, International Journal of Thermal Science 49 (2010) 1-9.

[19] S. M. Aminossadati, B. Ghasemi; Enhance natural convection in an isosceles triangular enclosure filled with a nanofluid, Computer and Mathematics with Applications 61 (2011) 1739-1753.

[20] Mostafa Mahmoodi; Numerical simulation of free convection of nanofluid in a square cavity with an inside heater, International Journal of Thermal Sciences 50 (2011) 798-805.

[21] Mostafa Mahmoodi; Numerical simulation of free convection in L-shaped cavities, International Journal of Thermal Sciences 50 (2011) 1731-1740.

[22] H. Sleh, R. Roslan, I. Hashim; Natural convection heat transfer in a nanofluid-filled trapezoidal enclosure, International Journal of Heat and Mass Transfer 54 (2011) 194-201.

[23] Omid Abouali, Coodarz Ahmadi; Computer simulations of natural convection of single phase nanofluids enclosures: A critical review, Applied Thermal Engineering 36 (2012) 1-13.

[24] Saleh, H., Basriati, S., and Hashim, I., Solutions of natural convection of nanofluids in a parallelogrammic enclosure by finite difference method, J. Mat. Dan Sains, 16(2)(2011), 77–81.

[25] Maxwell, J., 1904, A Treatise on electricity and Magnetism , 2nd ed., Oxford University, Cambridge.

[26] Salam H. Hussain and Ahmed K. Hussein; Natural convection heat transfer Enhancement in a differentially heated parallelogrammic enclosure filled with copper-water nanofluid, ASME-Journal of Heat Transfer, 136 (2014) 1-8.

Table (1): represent increase in heat transfer rate for different inclination angle and volume fraction along bottom heated wall at $Ra=10^6$ and 10^3.

$Ra=10^3$

Φ \ φ	0.05	0.1	0.15	0.2
60^o	13.5%	24.9%	34.4%	42.7%
30^o	13.5%	24.8%	35.8%	42.6%
0^o	13.5%	24.8%	34.4%	42.6%
-30^0	13.5%	24.8%	35.8%	42.6%
-60^o	13.5%	24.9%	34.4%	42.7%

$Ra=10^6$

Φ \ φ	0.05	0.1	0.15	0.2
60^o	10.4%	19.5%	27.4%	34.3%
30^o	7.6%	13.5%	18.9%	24.8%
0^o	8.3%	15.2%	21.1%	26.2%
-30^0	7.6%	13.5%	18.9%	24.8%
-60^o	10.4%	19.5%	27.4%	34.3%

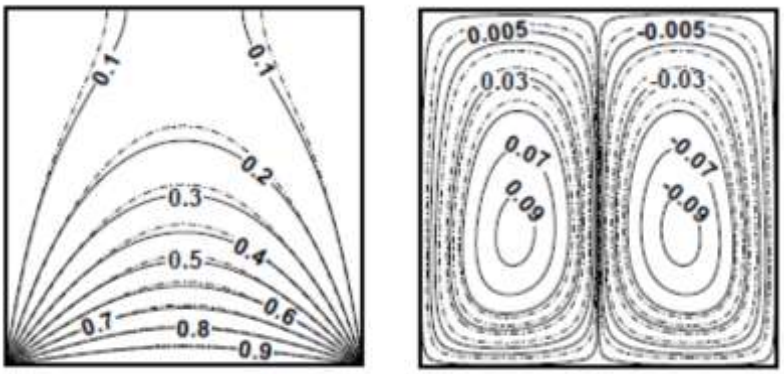

a. Present Work

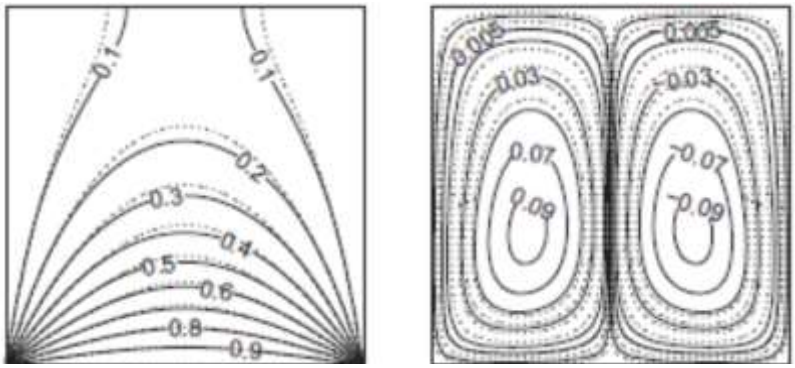

a. benchmark problem [4]

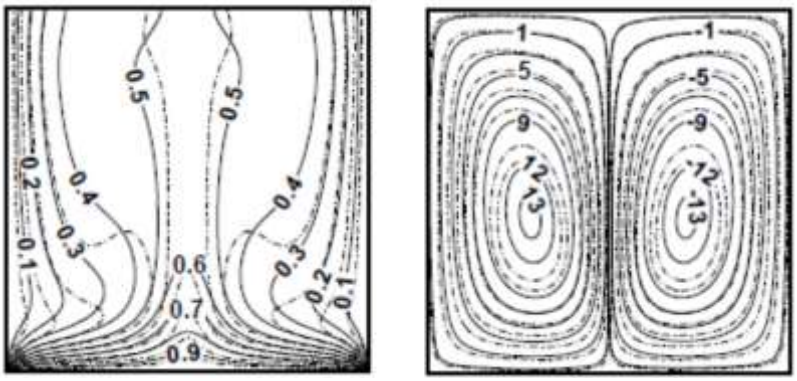

b. Present Work

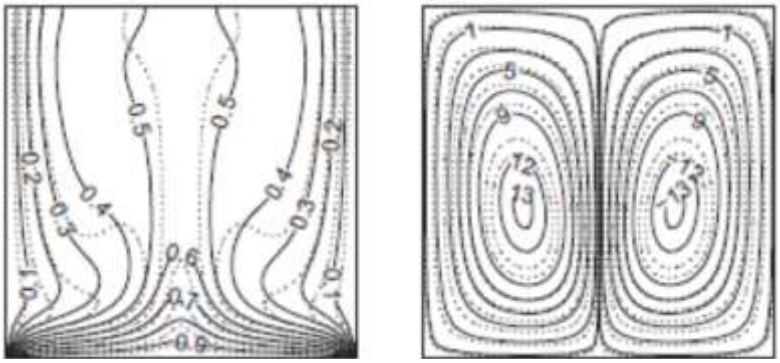

b. benchmark problem [4]

Figure (2): Comparison of temperature (θ) and stream function (ψ) contours for isothermally hot bottom and cold side walls of Cu–Water nanofluids with benchmark problem [4] for φ= 0.2 at (a) Ra = 10^3, (b) Ra = 10^5….., water and —, nanofluid.

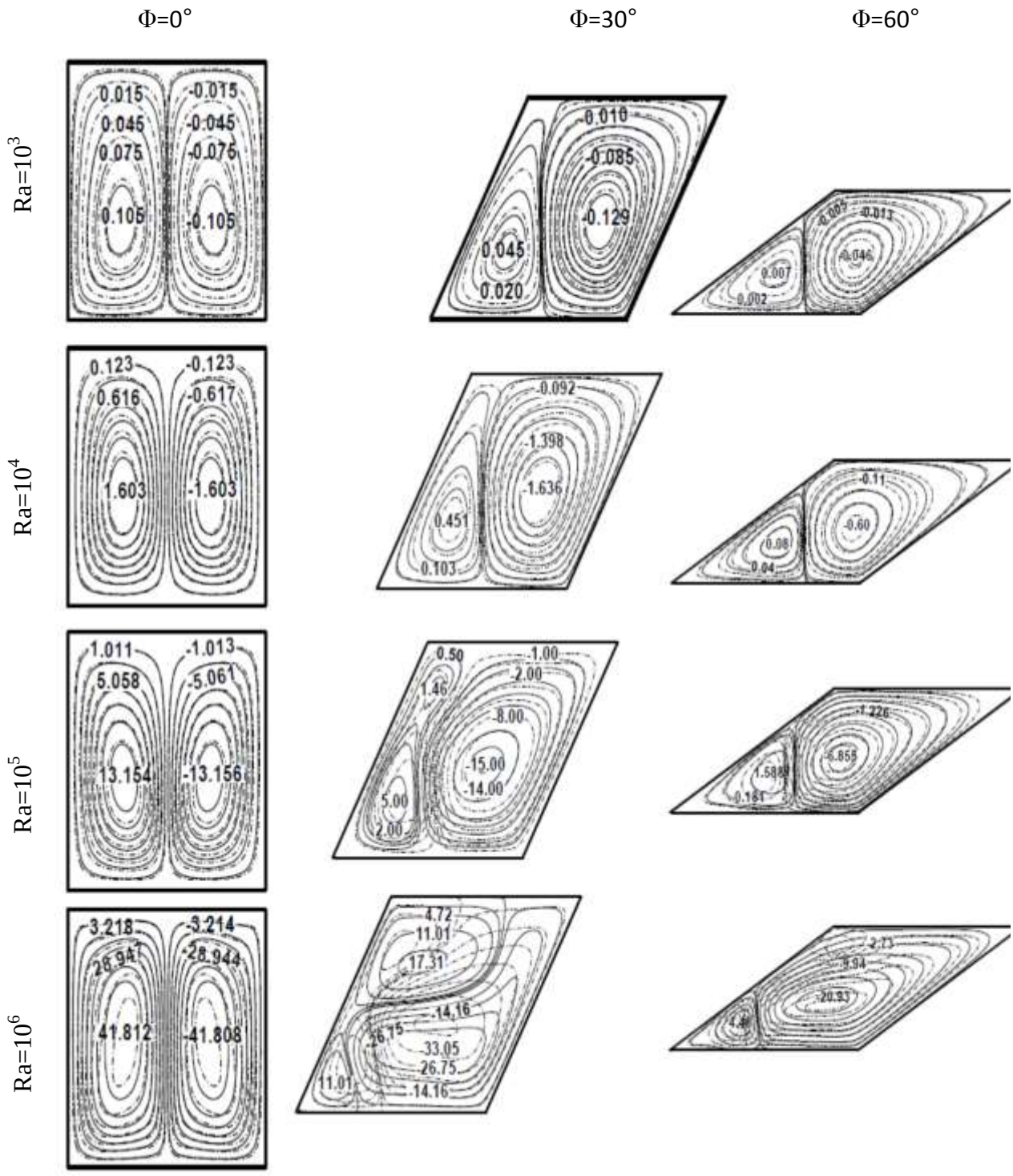

Figure (3): stream function (ψ) contours for isothermally hot bottom and cold side walls of Ag–Water nanofluids for different oblique angles (Φ) and Ra at φ= 0, ….., water and φ= 0.15,—,nanofluid.

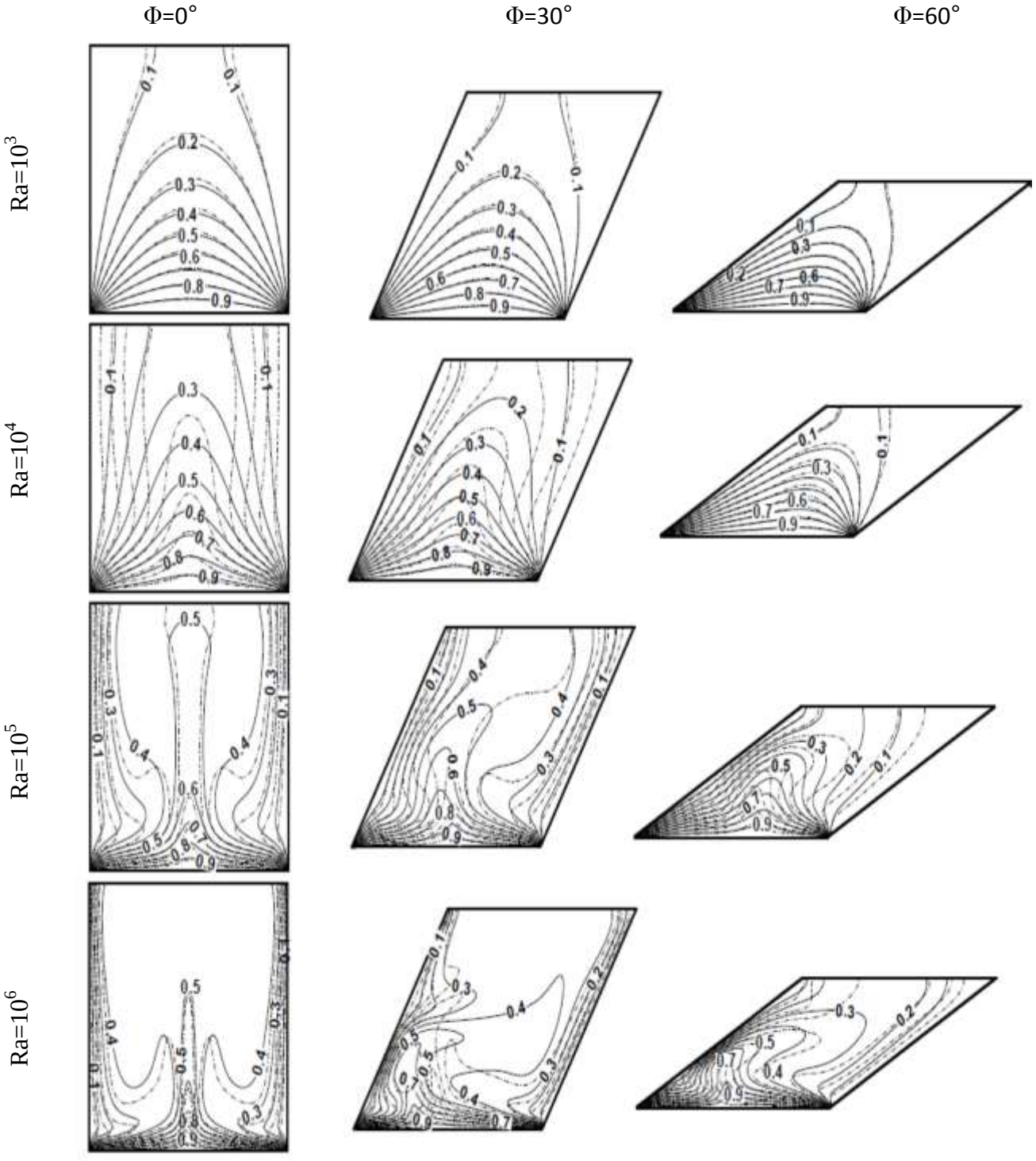

Figure (4): Temperature (θ) contours for isothermally hot bottom and cold side walls of Ag–Water nanofluids for different oblique angles (Φ) and Ra at φ= 0, ….., water and φ= 0.15,—,nanofluid.

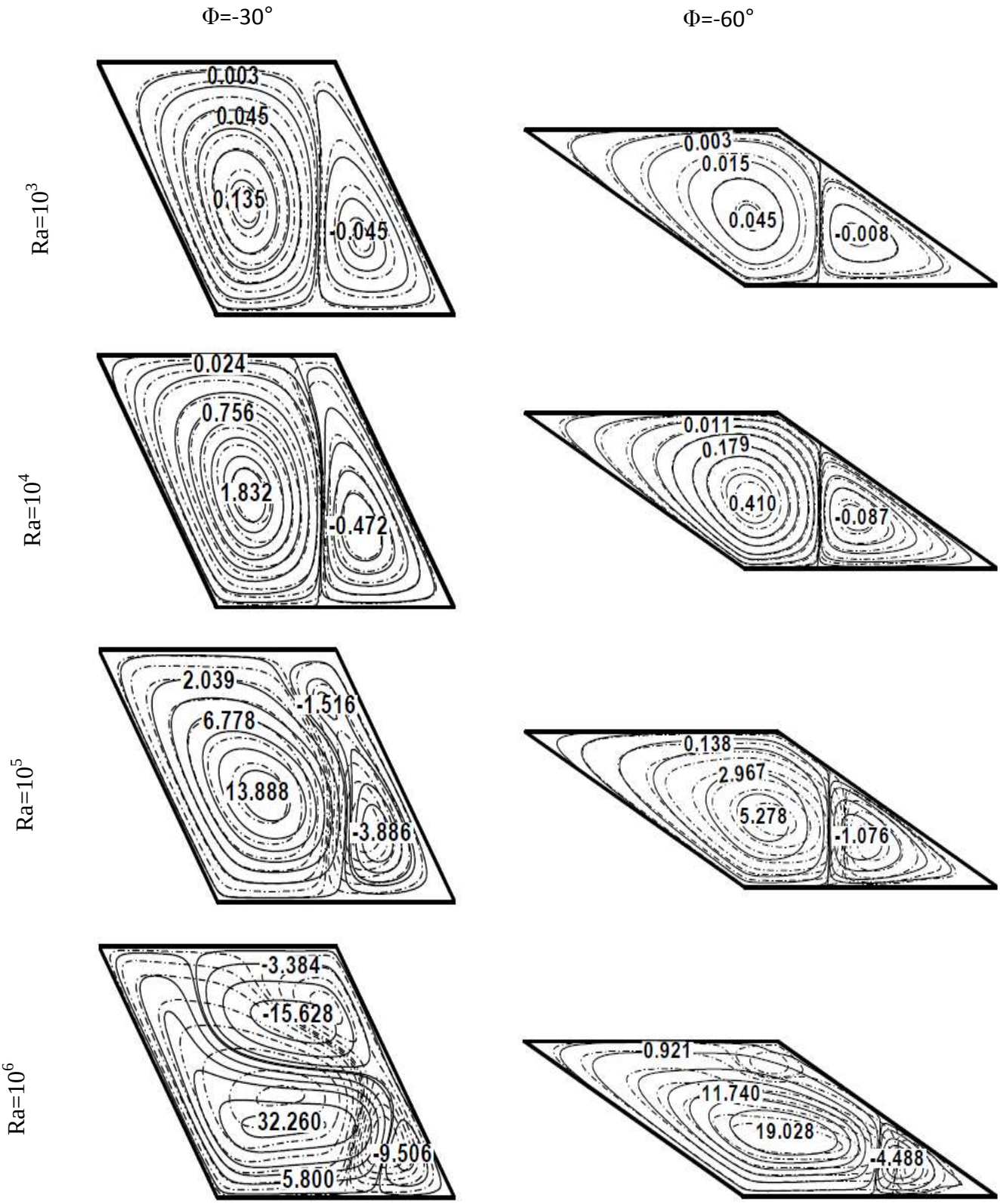

Figure (5): Stream function (ψ) contours for isothermally hot bottom and cold side walls of Ag–Water nanofluids for different oblique angles (Φ) and Ra at φ= 0, ….., water and φ= 0.15,—,nanofluid.

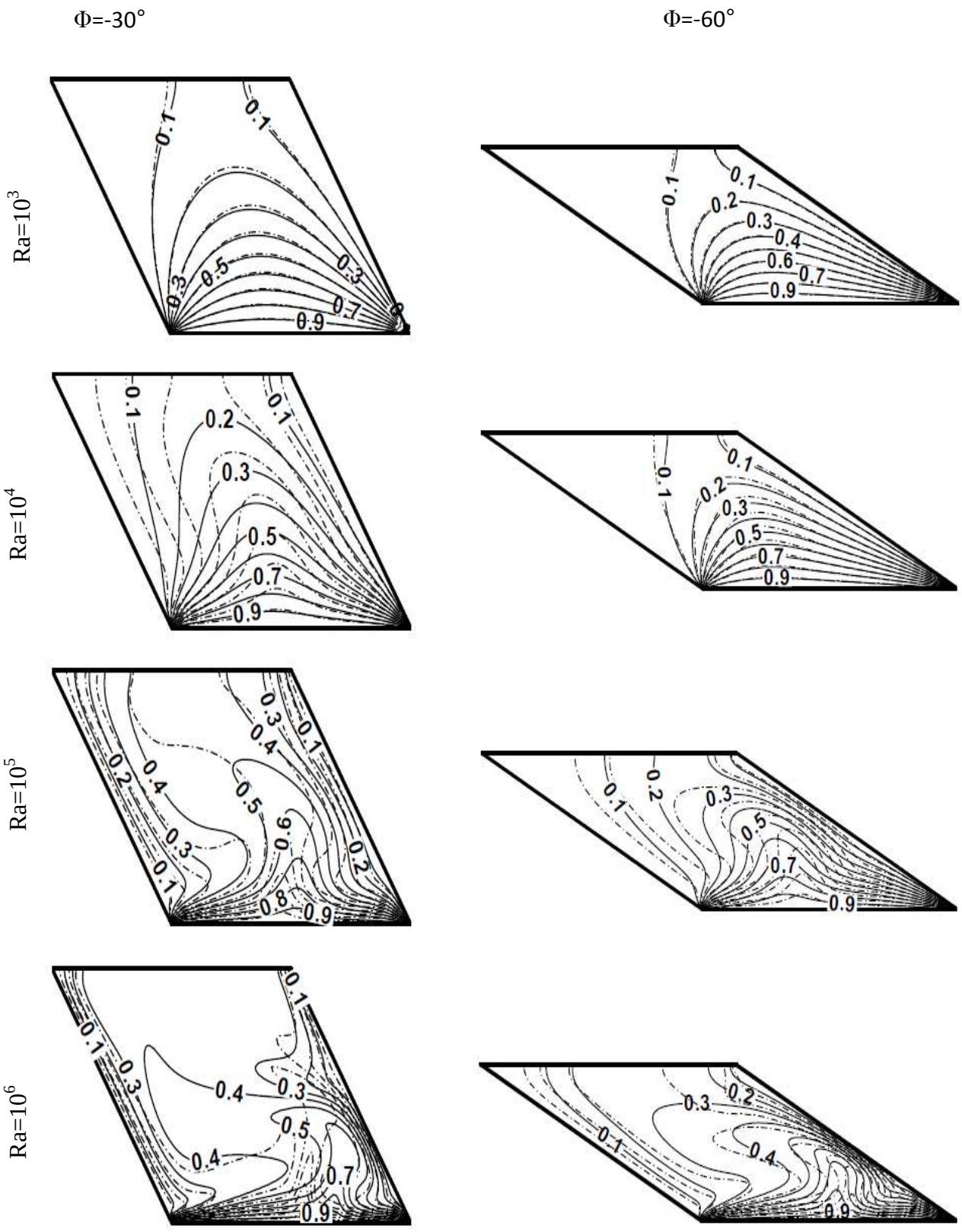

Figure (6): Temperature (θ) contours for isothermally hot bottom and cold side walls of Ag–Water nanofluids for different oblique angles (Φ) and Ra at φ= 0, …..., water and φ= 0.15,—,nanofluid.

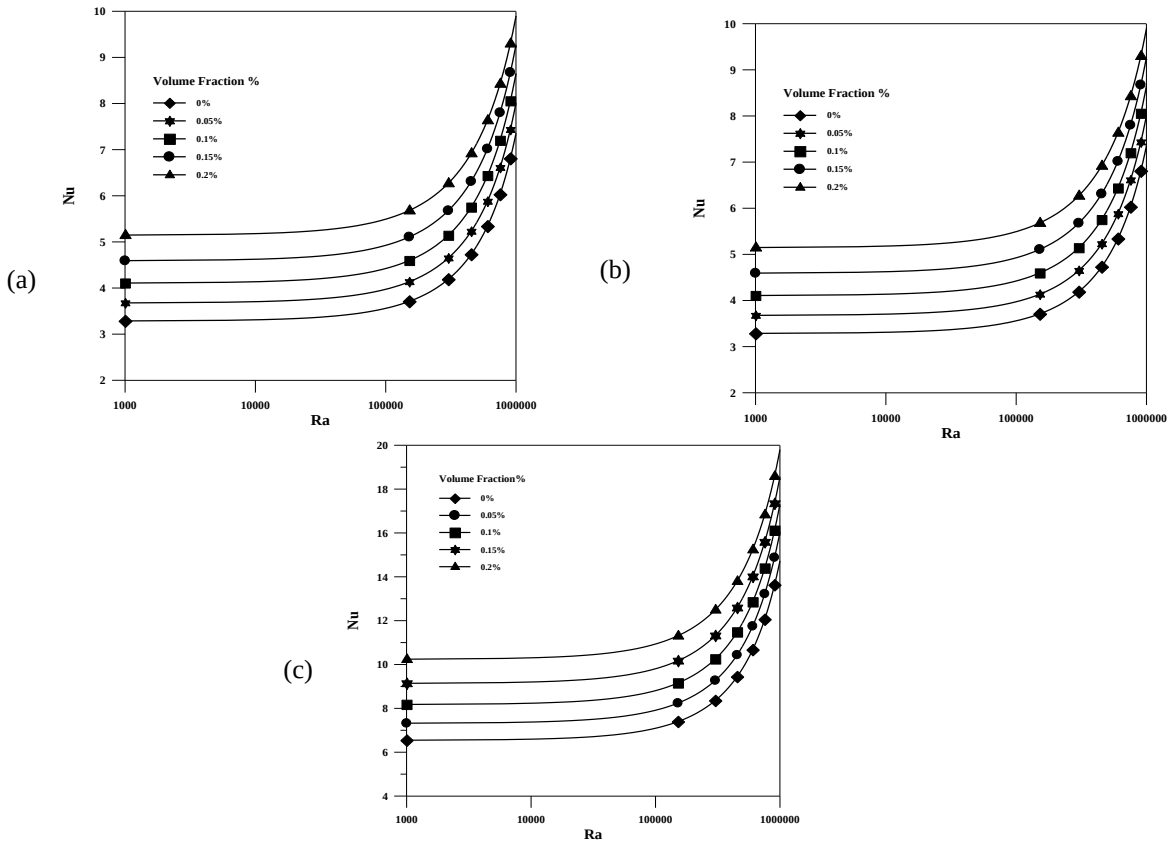

Figure (7): Average mean Nusselt numbers with Rayleigh numbers at different values of volume fraction and ($\Phi=0^o$) {(a)= left side wall, (b)= right side wall and (c)= bottom side wall}

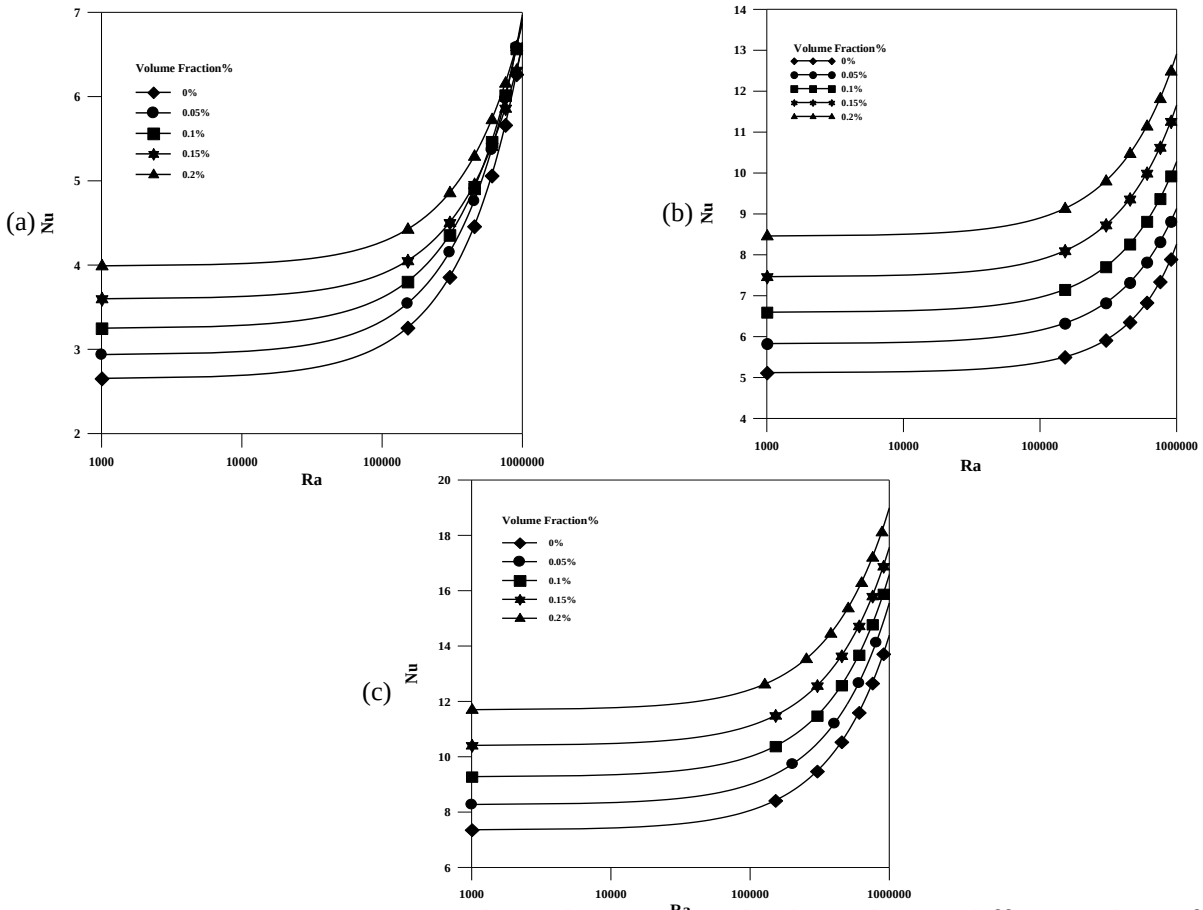

Figure (8): Average mean Nusselt numbers with Rayleigh numbers at different values of volume fraction and ($\Phi=30^o$) {(a)= left side wall, (b)= right side wall and (c)= bottom side wall}

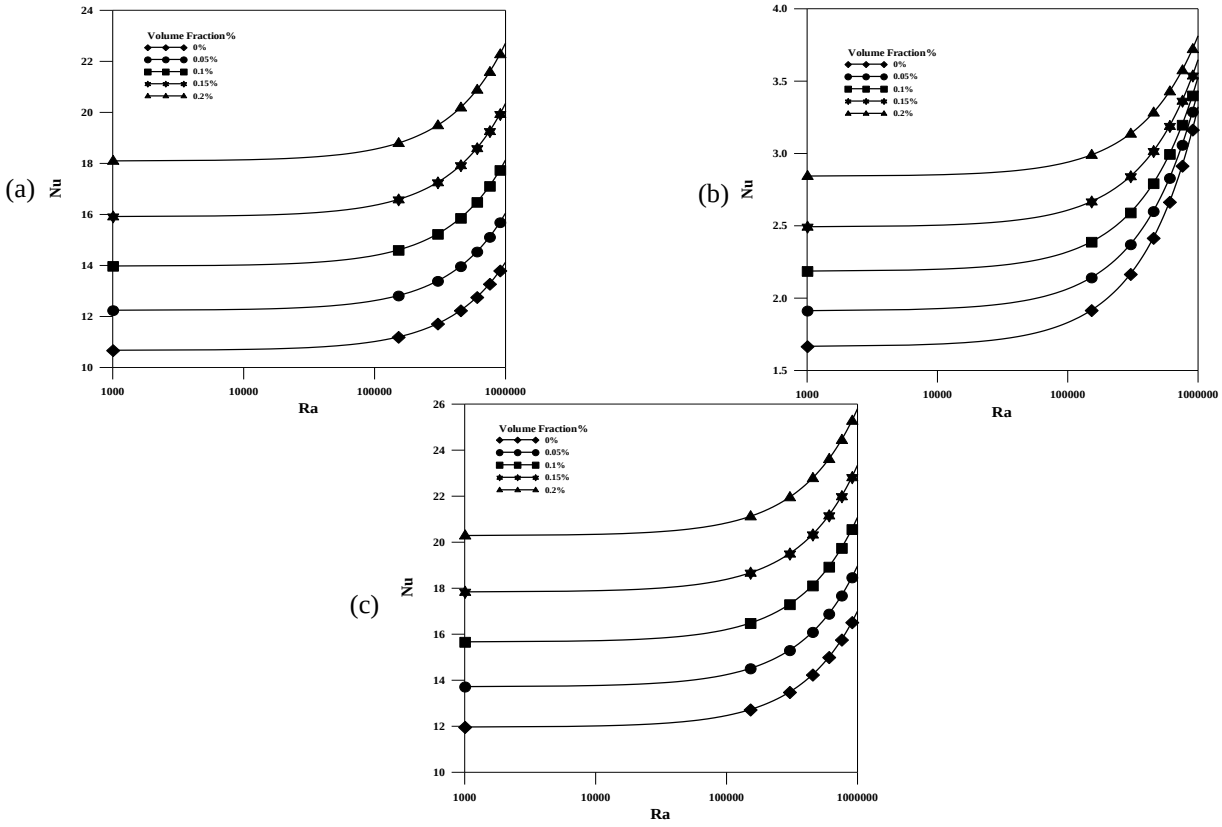

Fig (9) Average mean Nusselt numbers with Rayleigh numbers at different values of volume fraction and (Φ=60^o) {(a)= left side wall, (b)= right side wall and (c)= bottom side wall}

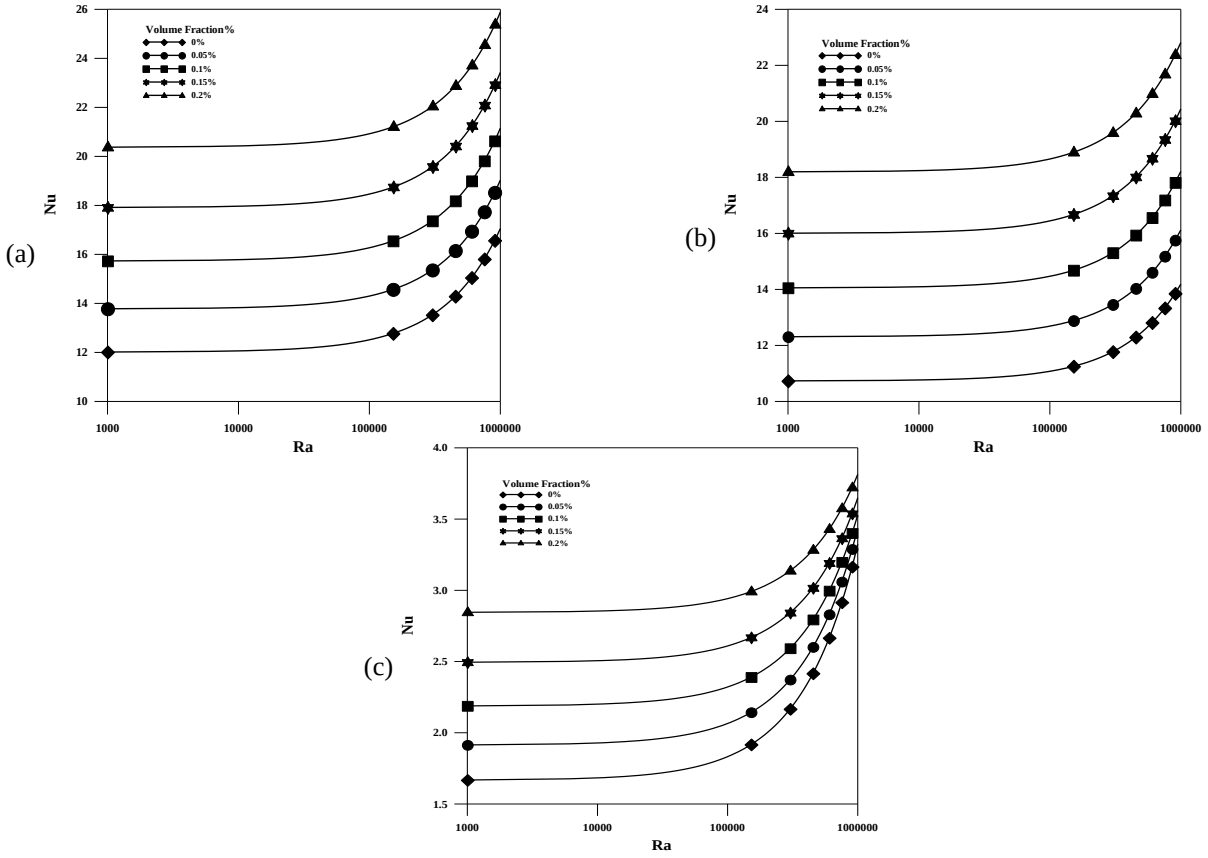

Figure (10): Average mean Nusselt numbers with Rayleigh numbers at different values of volume fraction and (Φ=-60^o) {(a)= left side wall, (b)= right side wall and (c)= bottom side wall}

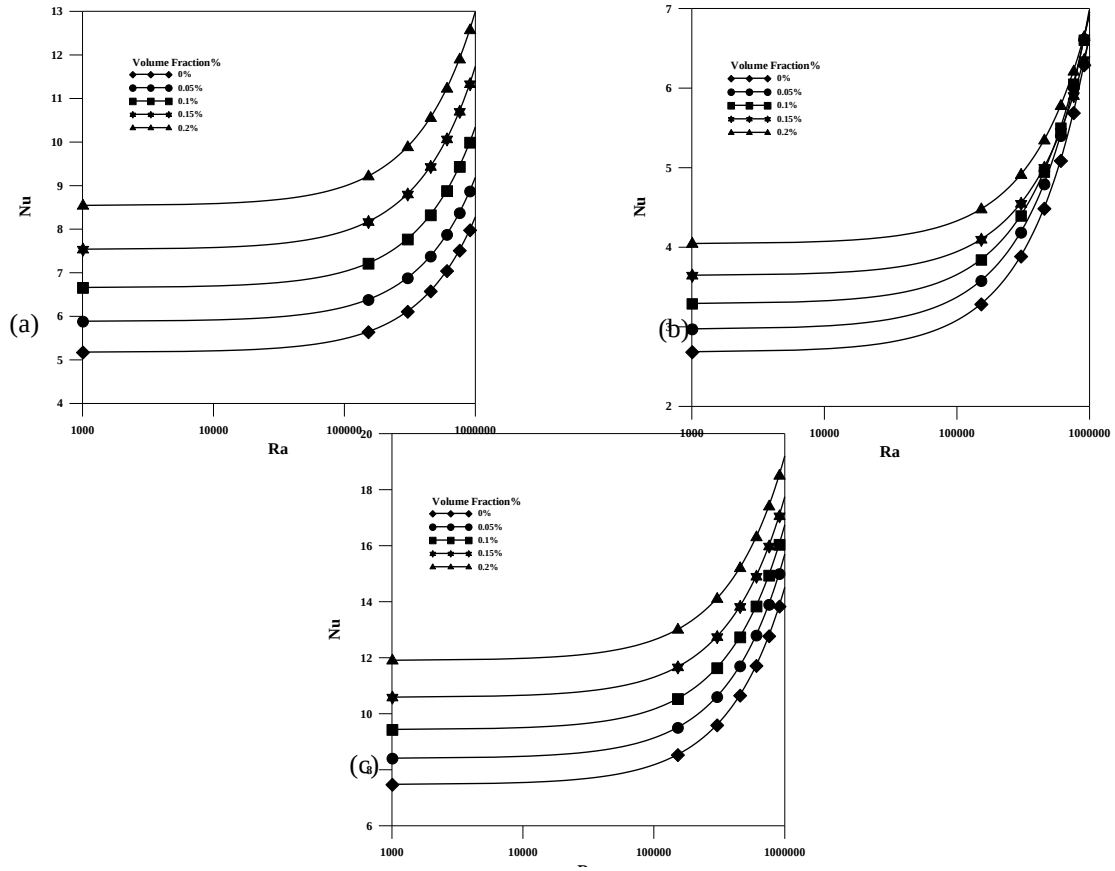

Figure (11): Average mean Nusselt numbers with Rayleigh numbers at different values of volume fraction and (Φ=-30^o) {(a)= left side wall, (b)= right side wall and (c)= bottom side wall}

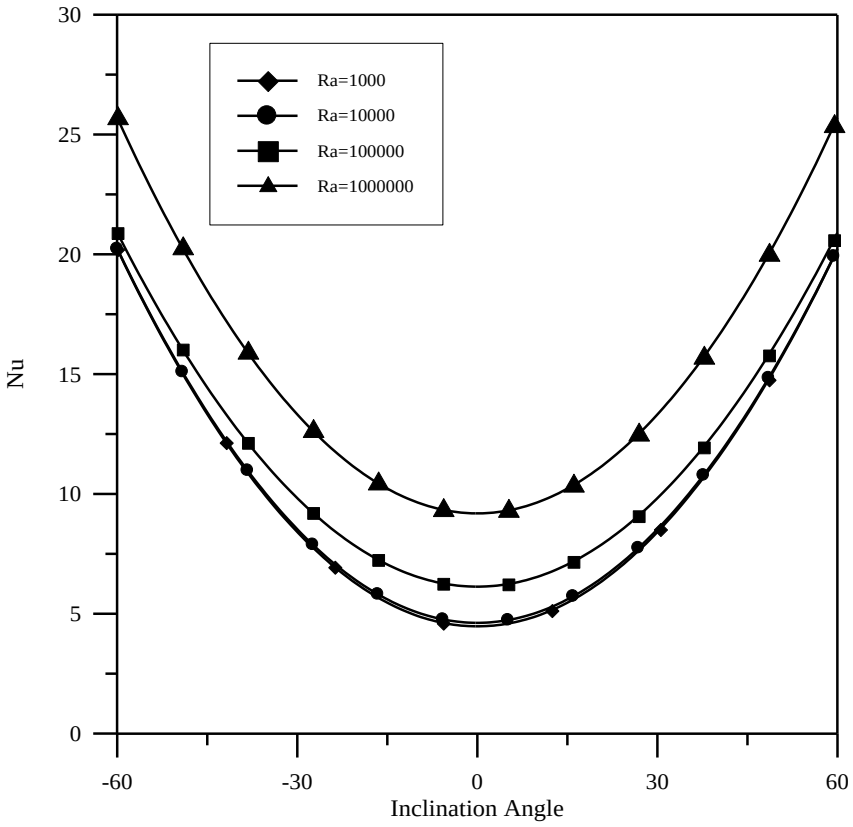

Figure (12) Average mean Nusselt numbers with Inclination angle at different values of Rayleigh numbers and (φ=0.2) for bottom heated wall}